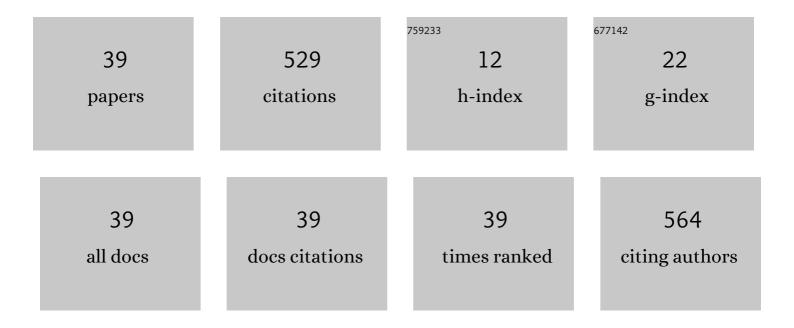
## Fa-Zhu Ding

List of Publications by Year in descending order

Source: https://exaly.com/author-pdf/5403956/publications.pdf Version: 2024-02-01



#	Article	IF	CITATIONS
1	High-Performance Ag-Modified Bi <sub>0.5</sub> Sb <sub>1.5</sub> Te <sub>3</sub> Films for the Flexible Thermoelectric Generator. ACS Applied Materials & Interfaces, 2020, 12, 7358-7365.	8.0	77
2	N-type Mg3Sb2-Bi with improved thermal stability for thermoelectric power generation. Acta Materialia, 2020, 201, 572-579.	7.9	60
3	Bi <sub>0.5</sub> Sb <sub>1.5</sub> Te <sub>3</sub> -based films for flexible thermoelectric devices. Journal of Materials Chemistry A, 2020, 8, 4552-4561.	10.3	53
4	Highly (00 <i>l</i> )-oriented Bi <sub>2</sub> Te <sub>3</sub> /Te heterostructure thin films with enhanced power factor. Nanoscale, 2018, 10, 20189-20195.	5.6	31
5	Enhanced flux pinning in MOD-YBCO films with co-doping of BaZrO3 and Y2O3 nanoparticles. Journal of Alloys and Compounds, 2012, 513, 277-281.	5.5	26
6	N-Type Mg <sub>3</sub> Sb <sub> 2- <i>x</i> </sub> Bi <i> <sub>x</sub> </i> Alloys as Promising Thermoelectric Materials. Research, 2020, 2020, 1219461.	5.7	26
7	Strong enhancement flux pinning in MOD-YBa 2 Cu 3 O 7â^'x films with self-assembled BaTiO 3 nanocolumns. Applied Surface Science, 2014, 314, 622-627.	6.1	23
8	Removal of CdTe in acidic media by magnetic ion-exchange resin: A potential recycling methodology for cadmium telluride photovoltaic waste. Journal of Hazardous Materials, 2014, 279, 597-604.	12.4	22
9	Bi2Te3-based flexible thermoelectric generator for wearable electronics. Applied Physics Letters, 2022, 120, .	3.3	21
10	Recent advances in flexible thermoelectrics. Applied Physics Letters, 2021, 118, .	3.3	16
11	Fabrication of high-JC BaTiO3-doped YBa2Cu3O7â^î^t thin films by the low-fluorine TFA-MOD approach. Journal of Alloys and Compounds, 2016, 664, 5-10.	5.5	13
12	Strong flux pinning enhancement in YBa <sub>2</sub> Cu <sub>3</sub> O <sub>7â^'<i>x</i></sub> films by embedded BaZrO <sub>3</sub> and BaTiO <sub>3</sub> nanoparticles. Chinese Physics B, 2013, 22, 077401.	1.4	12
13	Electrical and optical properties of ZnO:Al films with different hydrogen contents in sputtering gas. Rare Metals, 2015, 34, 173-177.	7.1	12
14	Microstructure and superconducting properties of (BaTiO3, Y2O3)-doped YBCO films under different firing temperatures. Rare Metals, 2017, 36, 37-41.	7.1	11
15	FEM analysis of piezoelectric film as IDT on the diamond substrate to enhance the quality factor of SAW devices. Diamond and Related Materials, 2020, 102, 107659.	3.9	11
16	An efficient approach for superconducting joint of YBCO coated conductors. Superconductor Science and Technology, 2022, 35, 075004.	3.5	11
17	Morphological evolution of CdS films prepared by chemical bath deposition. Rare Metals, 2013, 32, 380-389.	7.1	9
18	Study on Electromechanical Properties of Solder Jointed YBCO Coated Conductors With Etched Copper Stabilizer Under Axial Tension. IEEE Transactions on Applied Superconductivity, 2020, 30, 1-6.	1.7	9

#	Article	IF	CITATIONS
19	Enhancement in the critical current density of BaTiO <sub>3</sub> -doped YBCO films by low-energy (60) Tj ETQq	1,1,0.784	31,4 rgBT /O
20	Achievement of Low-Resistivity Diffusion Joint of REBCO Coated Conductors by Improving the Interface Connection of Ag Stabilizer. IEEE Transactions on Applied Superconductivity, 2021, 31, 1-7.	1.7	8
21	Bending properties of solder joint of YBCO coated conductors by etching copper stabilizer. Physica C: Superconductivity and Its Applications, 2019, 562, 42-47.	1.2	7
22	Heat treatment design of precursor solutions with different fluorine contents for YBa2Cu3O7â^'x films through the sol-gel approach. Journal of Sol-Gel Science and Technology, 2019, 90, 263-270.	2.4	7
23	One Structure, Two Elements—LuGe <sub>2</sub> Superconductor vs Ordinary Metallic Conductor LuSn <sub>2</sub> . A Case Study on How Site-Selective Germanium for Tin Atom Substitution Leads to Modulating of the Charge Distribution. Inorganic Chemistry, 2020, 59, 16853-16864.	4.0	7
24	Synthesis, characterization, and thermostability of bis(2,2,6,6-tetramethyl-3,) Tj ETQq0 0 0 rgBT /Overlock 10 Tf 5	0,542 Td 7.1	(5 <sub>5</sub> heptaned
25	Enhanced flux pinning of solution-derived YBa <sub>2</sub> Cu <sub>3</sub> O <sub>7â^'<i>x</i> </sub> nanocomposite films with novel ultra-small BaMnO <sub>3</sub> nanocrystals. Superconductor Science and Technology, 2019, 32, 025004.	3.5	5
26	Preparation of high performance YGdBCO films by low fluorine TFA-MOD process. Journal of Rare Earths, 2020, 38, 755-762.	4.8	5
27	Improved thermoelectric performance in n-type flexible Bi2Se3+x/PVDF composite films. , 0, , .		5
28	Substrate angle-induced fully c-axis orientation of AlN films deposited by off-normal DC sputtering method. Rare Metals, 2021, 40, 3668-3675.	7.1	5
29	Direct Cation–Cation Interactions Induced by Mg Dopants for Electron–Gas Behavior in α-Fe <sub>2</sub> 0 <sub>3</sub> . Journal of Physical Chemistry C, 2021, 125, 12893-12902.	3.1	5
30	Influence of BaZrO3 Amount on Microstructure and Properties inÂYBa2Cu3O7â^'x Films Prepared by TFA-MOD Process. Journal of Superconductivity and Novel Magnetism, 2011, 24, 1353-1356.	1.8	4
31	Effects of thickness on superconducting properties and structures of Y <sub>2</sub> O <sub>3</sub> /BZO-doped MOD-YBCO films. Chinese Physics B, 2015, 24, 057401.	1.4	4
32	Growth mechanism of CdS film prepared by chemical bath deposition. Rare Metals, 2014, 33, 324-329.	7.1	3
33	Precursor evolution and growth mechanism of BTO/YBCO films by TFA—MOD process. Chinese Physics B, 2014, 23, 107402.	1.4	2
34	Epitaxial growth of CaTiO3 buffer layer for fabrication of c-axis oriented YBCO film by sol-gel method. Journal of Sol-Gel Science and Technology, 2017, 82, 45-50.	2.4	2
35	Superconducting joining of YBCO coated conductors without a large critical current loss. Materials Today Physics, 2021, 21, 100567.	6.0	2
36	Synthesis, characterization, and thermostability of bis(2,2,6,6-tetramethyl-3,5-heptanedionato)barium(II). Rare Metals, 2013, 32, 67-74.	7.1	1

#	Article	IF	CITATIONS
37	Synthesis, characterization and thermostability of barium β-diketonate with tetraethylenepentamine ligand. Rare Metals, 2012, 31, 566-572.	7.1	о
38	Face Centered Cubic Co <sub>81.8</sub> Si <sub>9.1</sub> B <sub>9.1</sub> With High Magnetocrystalline Anisotropy. Physica Status Solidi - Rapid Research Letters, 2018, 12, 1700394.	2.4	0
39	High homogeneity 10 cm long BaTiO3-doped YBa2Cu3O7-δfilms by the trifluoroacetate metal-organic deposition process. Journal of Sol-Gel Science and Technology, 2020, 96, 297-303.	2.4	0